Description of the case study

During the night and early morning of the 14th of July 2011 the significant cloud layer expanding in the West of the country and slowly moving East produced precipitation and local storms. On the southern shores of the Baltic sea and in Pomerania region the precipitation was described as average to high. The rest of the country was covered by thin layer of clouds at that time. The minimal temperature recorded on the NE part of Poland reached 14°C, the maximum temperature was 19°C on the SW. Wind speed records show 60 km/h in the western regions of the country (during the storms up to 80 km/h) of E and SE direction turning to SW. The weather forecast estimated the precipitation within the storm areas up to 40 mm.

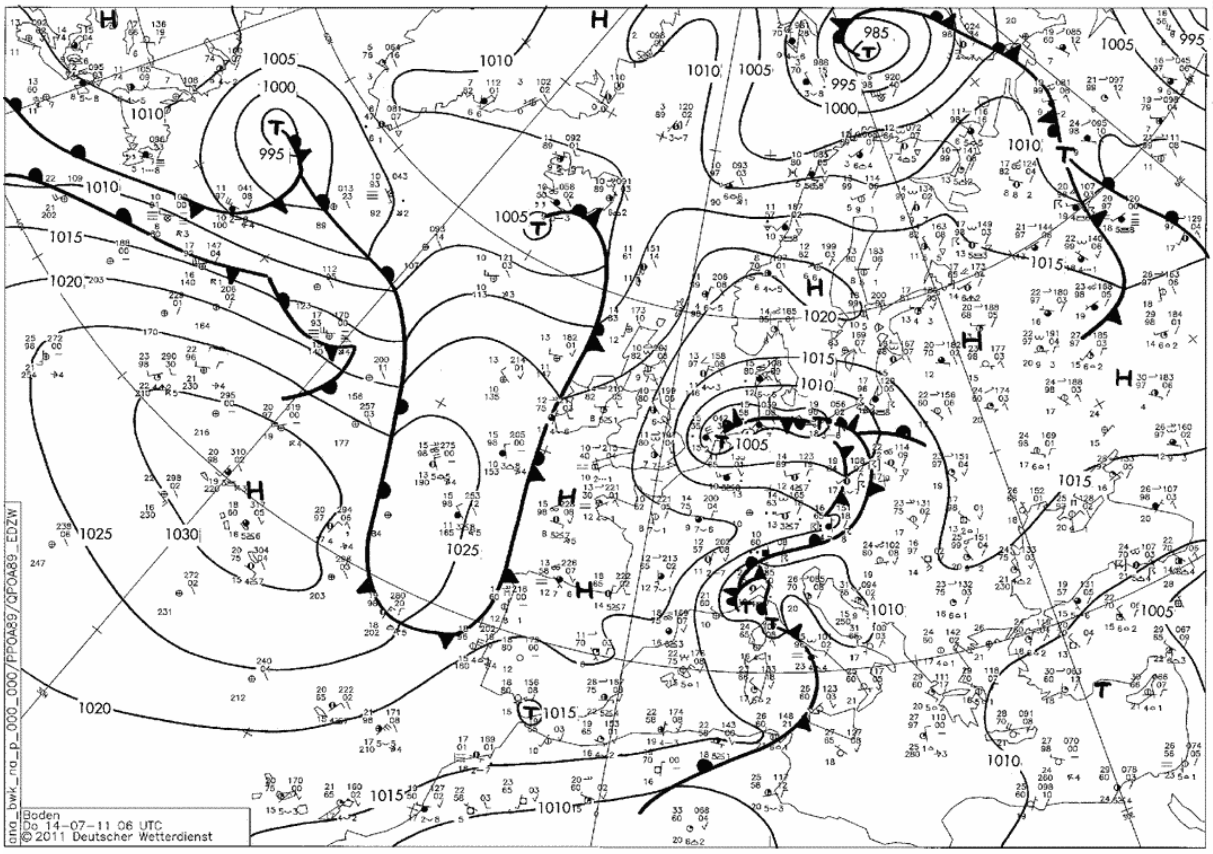

Fig.1 Synoptic chart at 0600 UTC on 14th of July 2011. Courtesy of Deutscher Wetterdienst.

Convective storms where observed over the country on that night and throughout a day. The precipitation was accompanied by lightning activity. On the Fig.2, the lightning activity map for twenty minutes time span (0550 UTC -0610 UTC) is presented (0557 UTC sensor overpass). The map was constructed on the base of data from Polish Lighting Detection System, PERUN.

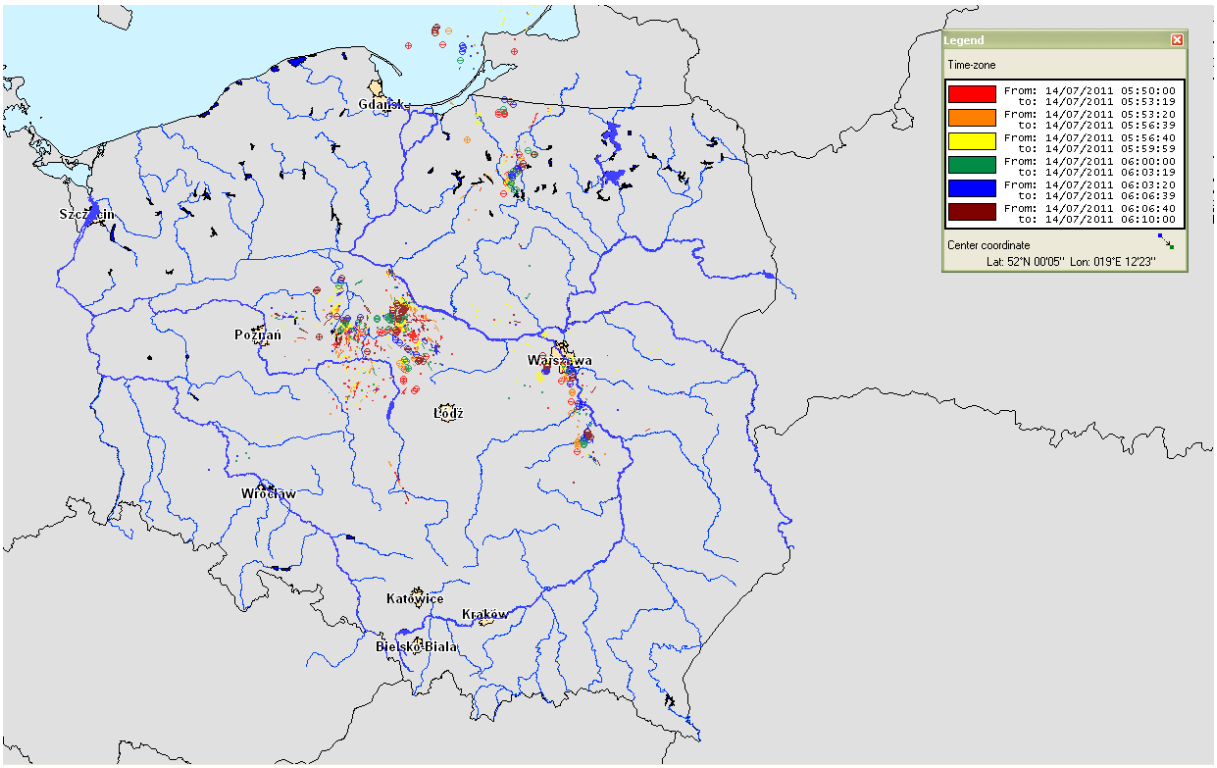

Fig.2 Total lighting map of Poland showing electrical activity between 0550 UTC - 0610 UTC on 14th of July 2011.

Vaisala lightning sensors installed in Poland detected 365 intra cloud events, 17 positive cloud-to-ground events and 243 negative cloud-to-ground events in the reference time period.

Data and products used

Reference data: data from Polish automatic rain gauges network (IMWM-NRI)
H-SAF product: PR-OBS-3
Ancillary data (used for case analysis):

- Polish meteorological radar network, POLRAD (IMWM-NRI)
- Polish Lighting Detection System, PERUN (IMWM-NRI)
- Weather charts (courtesy of Deutscher Wetterdienst)

Comparison

This event is dominated by convective systems of limited spatial scales moving across Poland. The highest peak measured by rain gauges is of about 9.6 mm/h, at the same time radar shows 54.0 mm/h while PR-OBS-3 shows a peak value of 14.2 mm/h.

On the Fig.3 the PR-OBS-3 product is visualized for the morning overpass. For comparison, the distribution of 10 minute precipitation obtained from RG and radar data measured at closest to the given time slot is presented. All precipitation maps were prepared using Nearest Neighbor method.

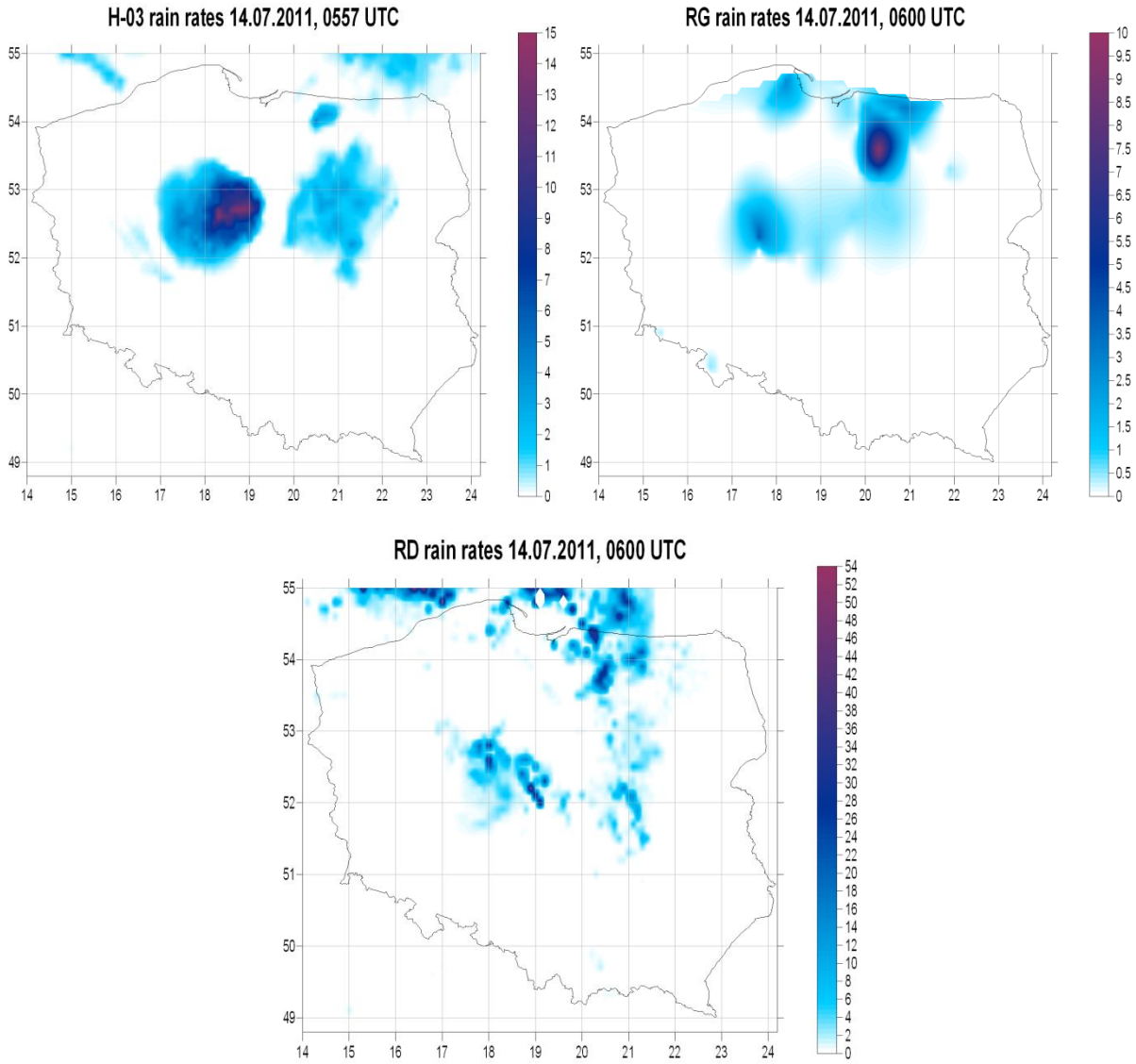

Fig.3 PR-OBS-3 at 0557 UTC on the 14th of July 2011 (left panel), 10 minute precipitation interpolated from RG data at 0600 UTC (right panel) and 10 minute precipitation derived from radar data at 0600 UTC (bottom panel). *Note diverse scale notation!*

On all maps, the precipitating areas reveal the lightning activity seen on the Figure 2. The general agreement between data sources visualizations was accomplished. The precipitating areas match each other with exception for the rain gauge map where maximum precipitation area present on both radar and H-03 satellite product was interpolated on sparse rain gauge network thus underestimated. On the other hand strong precipitating area over Olsztyn was underestimated by H-03.

Statistical scores

The results presented below were calculated on the satellite sub-dataset for which satellite pixels were attached to rain gauges. It means that precipitating satellite pixels which were not set in pairs with rain gauges (but are still present on the maps above) were excluded from this calculation.

The ability of PR-OBS-3 product to recognize the precipitation was analysed using dichotomous statistics parameters. The 0.25mm/h threshold was used to discriminate rain and no-rain cases. In the Table 1 the values of Probability of Detection (POD), False Alarm Rate (FAR) and Critical Success Ratio (CSI) are presented.

Table 1 Results of the categorical statistics obtained for PR-OBS-2 on the 14th July 2011

Parameter	Scores
POD	0.38
FAR	0.57
CSI	0.25

Higher value of FAR than the value of POD indicates that the product ability to recognize the convective precipitation is very low.

The quality of PR-OBS-3 in estimating the convective precipitation is presented on the Figure 4. The points on the scatter plot are mostly arranged above and below the diagonal, what indicates that PR-OBS-3 tends to overestimate light precipitation and underestimate the moderate one.

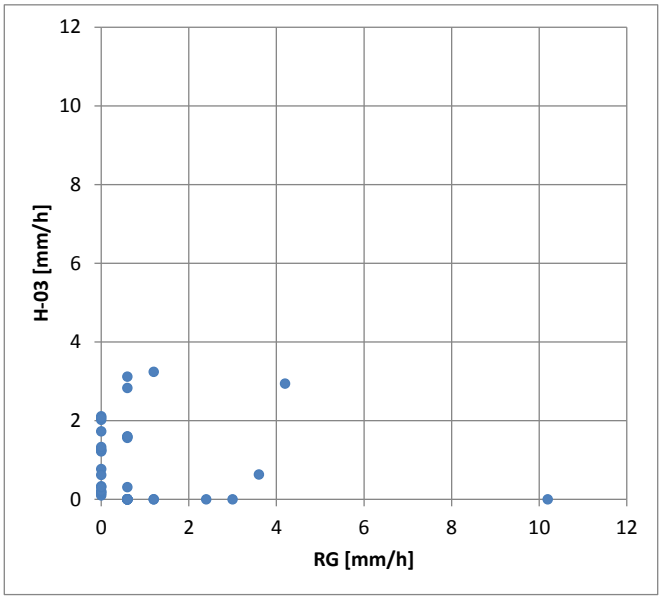

Fig.4 Scatter plot for measured (RG) and satellite derived (H-03) rain rate obtained for all PR-OBS-3 data on the 14th of July 2011

Finally, the analysis of rain classes was performed. The categories were selected in accordance with the common validation method. Figure 5 shows the percentage distribution of satellite derived precipitation categories within each precipitation class defined using ground measurements.

One can easily notice very poor ability of PR-OBS-3 to recognize the precipitation situations – in no rain area, 12 cases out of 16 was improperly allocated by satellite product. The light precipitation is not properly recognized in most cases – only 1 of 16 was recognized properly. When moderate is considered, the PR-OBS-3 quality is still bad: 2 out of 7 of the observed precipitation in this class are properly recognized.

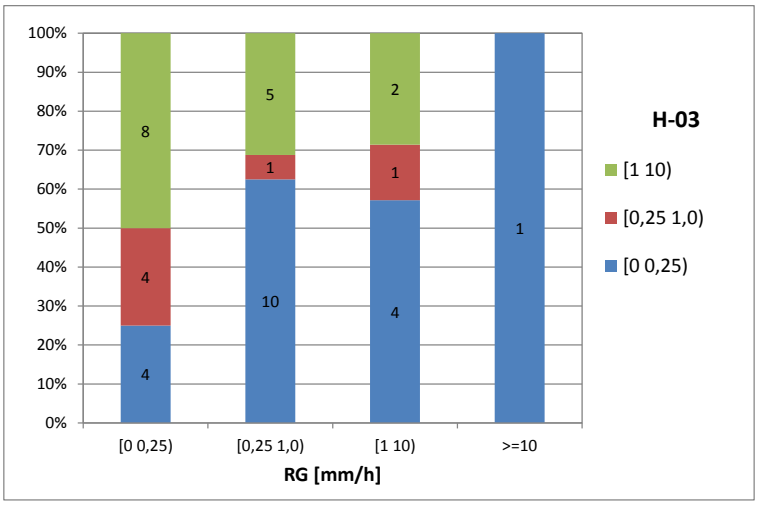

Fig.5 Percentage distribution of PR-OBS-3 precipitation classes in the rain classes defined using rain gauges (RG) data on the 14th of July 2011.

Some Conclusions

To sum it up, the analysis performed for situation with convective precipitation showed good ability of PR-OBS-3 product in recognition of precipitation spatial layout. Unfortunately, the satellite product underestimates moderate and overestimates light precipitation which shows its low skills in proper precipitation class recognition.

Only 25% of no rain class was properly recognized by H-03 in this case and the only heavy precipitation case was detected as no rain.